BORSE DI APPRENDISTATO SCIENTIFICO IN USA - BANDO CAIF 2020

Luca Orusa

Astronomy and Astrophysics Department, University of Chicago, 5640 South Ellis Avenue, Chicago, IL 60637

Abstract. Supervisor: Damiano Caprioli. The following report refers to the period that I spent at the University of Chicago between the 5th of September 2022 and the 5th of November 2022. I want to deeply thank ASI and CAIF for the opportunity that they gave me, that allowed me to have an incredible experience from a scientific point of view and increased a lot my expertise in astrophysics and plasma physics. The work was focused on the the study of particle acceleration in Supernova Remnants(SNR), astrophysical objects that are one of the main candidates to explain the primary cosmic rays in our Galaxy. The activities carried on will result in two upcoming papers.

Contents

1 General overview of the internship

The following report refers to the period that I spent at the University of Chicago between the 5th of September 2022 and the 5th of December 2022. The ASI-CAIF fellowship covered 2 months of the period, but I decided to extend my permanence for other 30 days. Here at the University of Chicago I worked under the supervision of Prof. Damiano Caprioli. I want to deeply thank ASI and CAIF for the opportunity that they gave me, that allowed me to have an incredible experience from a scientific point of view and increased a lot my expertise in astrophysics and plasma physics. As I will explain in this document, the work was focused on the the study of particle acceleration in Supernova Remnants(SNR), astrophysical objects that are one of the main candidates to explain the primary cosmic rays in our Galaxy, via numerical simulations and analitic computations. The activities carried on will result in two upcoming papers:

- L. Orusa, D. Caprioli, "Hybrid simulations of perpendicular shocks in the high Mach number regime": study of high Mach number perpendicular shocks via numerical simulations. In these three months this is the main project that I carried on, testing regions of the parameter space of supernova remnants shocks never explored before.
- L. Orusa, D. Caprioli, "The Theory of Shock Drift Acceleration at perpendicular shocks": this is a complementary paper that we are developing, with the aim of creating a complete theory for the acceleration process called shock drift acceleration.

To obtain all the results listed in this report, in this two months I learnt how to use the Fortran based codes dHybrid and dHybridR [1, 2], I learnt how to use for the first time in my career the language programming Matlab and I improved my knowledge of Mathematica. During the internship, besides of creating connections with several researchers of the University of Chicago, I also gave two seminars, during the AstroTuesday series and during the

Astronomy and Astrophysics Journal Club organized by Prof. Damiano Caprioli and Prof. Irina Zhuravleva. In November I was also able to visit Columbia University in New York to give a seminar, promoting the possibility that CAIF and ASI gave me.

2 Introduction

A long-lasting problem of Astroparticle Physics is the detection of sources responsible for the production of energetic cosmic rays (CRs). Authors of [3] proposed supernova remnants (SNRs) to be responsible for such accelerated particles, requiring about 10–30% of the kinetic energy of the SN ejecta to be converted into accelerated particles. This energetic motivation, combined with the acceleration mechanism proposed by Fermi [4], was the base on which was built the theory of diffusive shock acceleration (DSA), developed in the late '70s by several authors [5–7]. The most important result of the DSA mechanism is that the spectrum of the accelerated particles is predicted to be a universal power-law in momentum, with a spectral index that depends only on the shock compression ratio, defined as $r = \rho_2/\rho_1$, where $\rho_{1,2}$ is the density of particles upstream and downstream of the shock. Since for strong (i.e., large Mach number M_A) shocks the compression ratio points towards the asymptotic value of $r = 4$, particles are expected to be accelerated with a spectrum $f(p) \propto p^{-3r/(r-1)} \propto p^{-4}$, with p the modulus of the particle momentum (see, e.g., [7]). The spectrum of Galactic CRs observed at Earth is measured to be a power-law $\propto E^{-2.7}$ from a few GeV up to a few times 10^6 GeV for protons, energy limit that has to be multiplied by an additional factor Z for heavier nuclei with charge Z. The discrepancy between the spectrum predicted by DSA ($\propto E^{-2.0}$ in energy for relativistic particles) and the measured one can be explained considering that CR in their propagation in the Galaxy are affected by a diffusion process, that can be modelled as $D(R) \propto R^{-\delta}$ where R is the rigidity of the particle. Combining the two spectra it is possible to find a compatibility between models and observations. Understanding particle acceleration process at non-relativistic shocks, and the conditions that may favor it, is not a problem limited to SNRs, though. Most astrophysical shocks are collisionless, which means that energy and momentum conversion is not performed by collisions of particles, but is mediated by collective electromagnetic processes. There are many examples of collisionless shocks in addition to SNR ones, in a very wide range of scales: in the Solar System (for example the Earth's bow shock or the solar-wind-related shocks), in the jets of active galaxies, and also in clusters of galaxies. These shocks are characterized by a wide range of sonic Mach numbers, magnetization, and relative inclination between the shock velocity and the unperturbed magnetic field, but they are usually associated with the presence of accelerated particles. Often astrophysical shocks are also connected to magnetic fields much larger than the interstellar ones, up to levels that cannot be explained by the simple compression between upstream and downstream density. For example, X-ray observations of young SNRs report the detection of a magnetic fields of a few hundreds μG, a factor of 50–100 bigger than in the interstellar medium [8, 9]. These amplified fields are probably produced by accelerated ions through different plasma instabilities [10]. CR spectra, acceleration efficiency and magnetic field amplification in astrophysical shocks can be calculated using a two-fluid approach [11], with Monte Carlo simulations [12–14], or solving the CR transport equation either numerically [15], or analytically [16]. These methods produce coherent results and can properly describe the large scale dynamics of the shock. Nevertheless, they need to be corrected with the physics at small scale that describe the particle dynamics and the excitation of the magnetic turbulence. To overcome these limitations and to coherently take

into account of the highly non-linear relation between particles and electromagnetic fields, numerical kinetic simulations are necessary. Such simulations of non-relativistic collisionless shocks have been carried out both in the full particle-in-cell (PIC) approach [17], or in the hybrid (kinetic ions–fluid electrons) approach [18]. With respect to PIC simulations, the hybrid approach does not resolve the small electron plasma scales. Therefore it is possible to simulate more macroscopic systems without losing important information about the shock dynamics, which is basically dominated only by ions. Trough the self-consistent treatment of the relation between accelerated particles and electromagnetic fields it is possible to study the correlation between ion acceleration and magnetic field amplification.

3 Project

3.1 Introduction: perpendicular shocks

During this internship I explored in particular the high Mach number perpendicular shocks regime, finding extremely important results for the scientific community. Perpendicular shocks characterize several astrophysical objects, from SNRs to Galaxy clusters to solar wind, and so far in literature no ion acceleration have been detected in self consistent simulations, which is inconsistent with the detection of a radio emission from some SNRs characterized by this type of configuration of the magnetic field. These shocks have angles $\sim 90°$ between the direction of motion of the shock and the background upstream magnetic field. The structure of perpendicular shocks in the supercritical regime ($M_A > M_{A*}$, where $M_{A*} \sim 3$) has not been extensively explored in the past. The shock structure can be describe in this way: a fraction of the incoming ions are reflected at the shock front (namely the 'ramp') and the reflected ions form a slightly dense region, referred to as the 'foot', in front of the ramp. The ions also accumulate immediately behind the ramp and generate an extremely strong magnetic field there, which is called the (magnetic) 'overshoot'. In the past one-dimensional (1D) PIC simulations have been performed to investigate high-M_A perpendicular shocks [19]. Also several two-dimensional (2D) simulations have been performed [20]. However, most simulations have been conducted for relatively low M_A number (<15). It is worth then to perform simulations for stronger shocks, to see how the dynamics of particles change and what type of plasma magnetic turbulence dominates.

3.2 Simulation setup

I have performed two and three dimensional simulations of non-relativistic shocks with different M_A, with an orientation of the initial magnetic field of 80°(quasi-perpendicular shocks) oriented in the xy plane. The presented simulations cover an unprecedentedly tested M_A regime. The simulations in this report are performed with the dHybrid code, a massively parallel, non-relativistic, hybrid code. Ions are treated kinetically and electrons as a neutralizing fluid, with a prescribed polytropic equation of state. Lengths are measured in units of the ion skin depth c/ω_p, where c is the light speed and $\omega_p = \sqrt{4\pi ne^2/m}$ is the ion plasma frequency, with m, e and n the ion mass, charge and number density, respectively. Time is measured in inverse cyclotron times $\omega_c^{-1} = mc/eB_0$, with B_0 the strength of the initial magnetic field. Finally, velocities are normalized to the Alfvén speed $v_A = B/\sqrt{4\pi mn} = c\omega_p/\omega_c$. All simulations include the three spatial components of the particle momentum, and the three components of electric and magnetic fields. In these simulations v_{sh} is the upstream fluid ve-

locity in the downstream reference frame. The initial magnetic field $B_0 = B_0\mathbf{x}$ is not in the same direction of $v_{sh} = -v_{sh}\mathbf{x}$, but is oriented with an angle of 80°. Ions are initialized with thermal velocity $v_{th} = v_A$, so that their temperature reads $T_0 = \frac{1}{2}mv_A^2/k_B$, with k_B the Boltzmann constant. Electrons are initially in thermal equilibrium with ions, i.e., $T_e = T_i = T_0$, and their adiabatic index is chosen in such a way to reproduce the expected jump conditions at the shock. The sound of speed is $c_s = \sqrt{2\gamma k_B T_0/m}$ and hence the sonic Mach number reads $M_s = M_A\sqrt{\gamma}$, with $\gamma = 5/3$ the ion adiabatic index. This regime is typical of the cold interstellar medium: with $n = 0.1$ cm^{-3}, $B_0 = 3\mu G$ and $T = 10^4$ K one has $v_A \sim c_s \sim 15$ km s^{-1}. Except when otherwise specified, throughout the report I indicate the shock strength simply with $M = M_A \sim M_s$. The shock is produced by sending a supersonic flow against a reflecting wall (left side in figures); the interaction between the initial stream and the reflected one produces a clear discontinuity, which propagates to the right in the figures. As a consequence, in the simulation the downstream fluid is at rest, and the kinetic energy of the upstream flow is converted into thermal energy at the shock front.

3.3 2D simulations: first results

I started the project performing 2D simulations with different M_A, in order to study the variation of the magnetic amplification with this parameter, and to see if acceleration of ions can start in high M_A number perpendicular shocks, phenomena not detected for M_A<100 in 2D. I pushed the code up to M_A=2000, region never explored in literature. I perfomed simulations in box of size [2000,50] c/ω_p, after that I checked that the results do not change varying the transverse size. I also performed a convergence test changing the resolution of the simulations(number of cells of the grid used for the box), reaching a saturation of the results for 2.5 cells per c/ω_p. If Fig. 1 I report the magnetic field amplification(left) and the particle spectrum(right) for M_A=100. On average the magnetic field is amplified in the downstream region by a factor of ~ 15, up to 30 for the overshoot, while no particle acceleration is observed, with all the ions characterized by thermal or supra-thermal energies. The results are reported for $t = 36\omega_c^{-1}$. The evolution of she shock at later times does not change the results.

In Fig. 2 I report the same plots as 1, but for M_A=500. It is clear how in the high M_A regime the simulation produce a shape of the magnetic field not homogeneous as in Fig. 1, and that the structure described in Section 3.1 is broken.

I performed the same type of simulations also for M_A=5,10,20,60 and 2000, in order to study the dependence with M_A. In the next section, I try to explain the mechanism of magnetic field amplification and see if it is consistent with the standard magneto-hydrodinamics(MHD) interpretation. One of the most important results of this initial tests is that, a part of producing an amplified magnetic field, no particle acceleration is detected.

3.4 Shock hydrodinamics

Several works have developed a MHD theory of CR-modified shocks including the dynamical role of energetic particles, as well as of the self-generated magnetic field [21, 22]. To understand if MHD is self-consistent for these type of shocks, I consider the conservation equations for mass, momentum, and energy in a 1D(in higher dimensions the simple analitic calculation

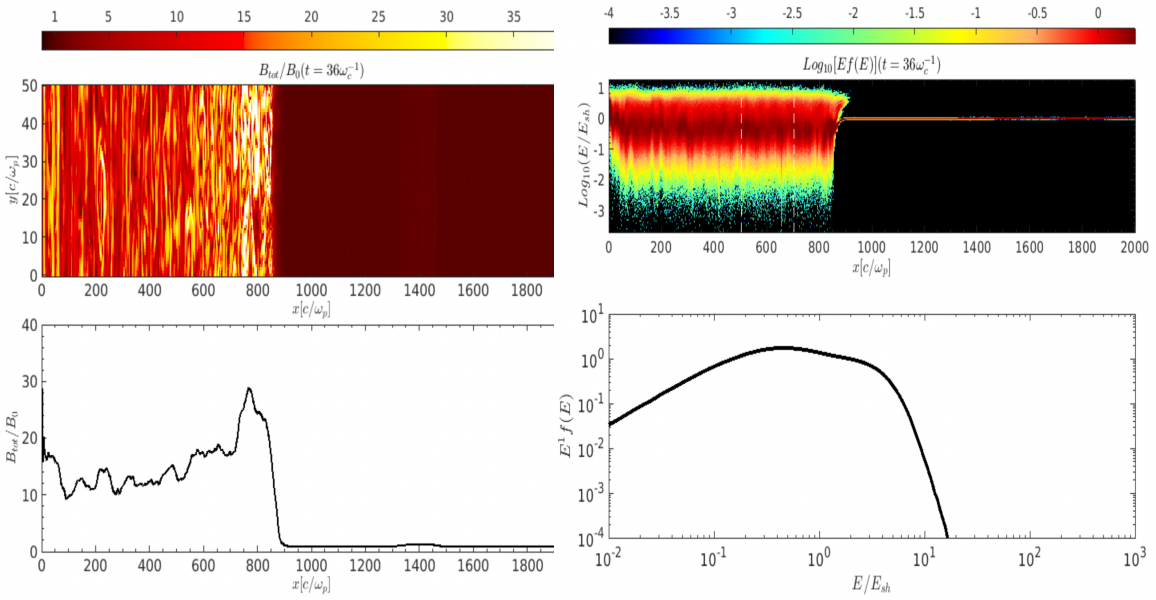

(a) (b)

Figure 1: The magnetic field amplification(left) and the particle spectrum(right) for M_A=100. On average the magnetic field is amplified in the downstream region by a factor of ~ 15, up to 30 for the overshoot, while no particle acceleration is observed, with all the ions characterized by thermal energies. The results are reported for $t = 36\omega_c^{-1}$. Evolution of she shock at later time does not change the results.

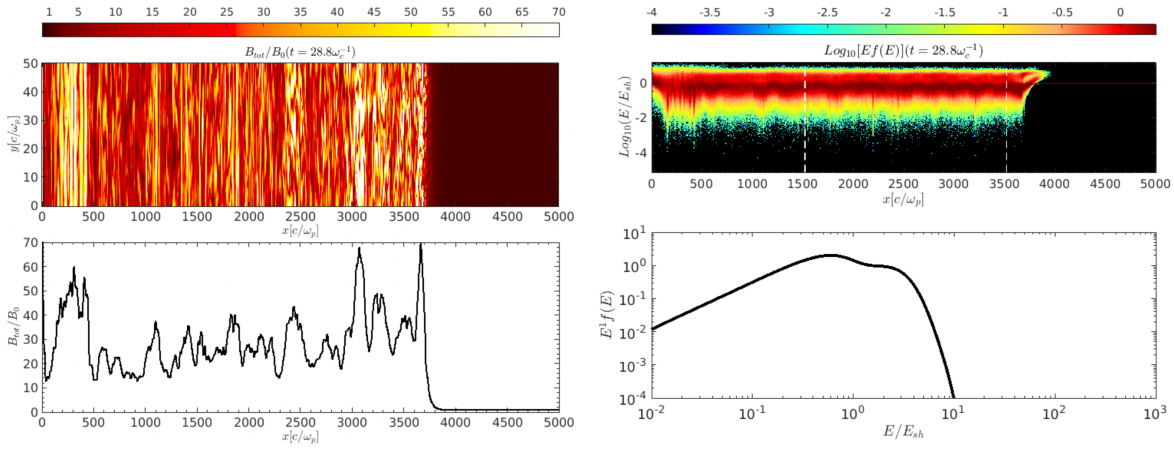

(a) (b)

Figure 2: The magnetic field amplification(left) and the particle spectrum(right) for M_A=500. On average the magnetic field is amplified in the downstream region by a factor of ~ 30, up to 55 for the overshoot, while no particle acceleration is observed, with all the particles characterized by thermal energies. The results are reported for $t = 36\omega_c^{-1}$. Evolution of she shock at later time does not change the results.

proposed can't be performed), non-relativistic, stationary, shock:

$$[\rho u] = 0 \tag{3.1}$$

$$\left[\rho u^2 + P_g + P_c + P_B\right] = 0 \tag{3.2}$$

$$\left[\frac{1}{2}\rho u^3 + F_g + F_c + F_B\right] = 0 \tag{3.3}$$

where γ_i, P_i, and F_i are the adiabatic index, pressure, and energy flux of thermal gas, CRs, and magnetic fields ($i = g, c, B$, respectively). The bulk flow velocity is defined as $\mathbf{u} \equiv -u\mathbf{x}$; the square brackets denote the difference between two arbitrary x locations. With appropriate prescriptions for F_i, this set of equations can be used to solve for the shock jump conditions. Since there is not CR acceleration in the previous simulations, all the quantities with subscript c are set to 0. The thermal gas energy flux has the canonical form:

$$F_g(x) = \frac{\gamma_g}{\gamma_g - 1} u(x) P_g(x). \tag{3.4}$$

The "magnetic" energy flux, in general, has contributions from both the magnetic pressure and the kinetic energy associated with the plasma fluctuations and can be described effectively with the same formula written in 3.4, with the presence of a γ_B=1.5 for Alfvénic fluctuations. This is the prescription that is adopted in the absence of a general theory.

Considering Equations 3.2 and 3.3 between 0 (far upstream) and 2 (downstream, in the 'overshoot' region), normalizing the momentum(energy) flux equation and dividing by the ram pressure (energy) $\rho_0 u_0^2$, $(\rho_0 u_0^3/2)$, it is possible to introduce the normalized pressure $\xi_i \equiv P_{i,2}/(\rho_0 u_0^2)$ and $\eta_i \equiv 2\gamma_i/(\gamma_i - 1)$, obtaining:

$$\xi_g \simeq 1 + \frac{1}{\gamma_g M_s^2} + \frac{1}{2M_A^2} - \frac{1}{R_{tot}} - \xi_B \tag{3.5}$$

and

$$1 + \frac{\eta_g}{\gamma_g M_s^2} + \frac{3}{M_A^2} \simeq \frac{1}{{R_{tot}}^2} + \frac{\eta_g \xi_g}{R_{tot}} + \left(\frac{2u_{B,2}}{u_2} + 1\right)\frac{2\xi_B}{R_{tot}}, \tag{3.6}$$

where $M_s \equiv \rho_0 u_0^2/\gamma_g P_0$, $M_A \equiv 4\pi\rho_0 u_0^2/B_0^2$ and R_{tot} are the far upstream sonic and Alfvénic Mach numbers and the compression factor, respectively. As outlined in [22] $u_{B,2}$ can be written as:

$$u_{B,2} = u_2(1 + \sqrt{2R_{tot}\xi_B}). \tag{3.7}$$

where R_{tot} is the total compression ratio. R_{tot} can be found by combining equations 3.5, 3.6, and 3.7. The equations can be rewritten into a single quartic equation in terms of $X = \sqrt{R_{tot}}$ where the coefficients depend on M_s, M_A and the post-shock pressure ξ_B, namely:

$$c_1 X^4 + c_2 X^3 + c_3 X^2 + c_4 = 0; \tag{3.8}$$

with the coefficients:

$$\begin{aligned}
c_1 &= 1 + \frac{\eta_g}{\gamma_g M_s^2} + \frac{3}{M_A^2} \\
c_2 &= -\sqrt{2\xi_B}\,(4\xi_B) \\
c_3 &= \eta_g(\xi_B - 1 - \frac{1}{\gamma_g M_s^2} - \frac{1}{2M_A^2}) - 6\xi_B \\
c_4 &= \eta_g - 1.
\end{aligned}$$

with $\gamma_g = 5/3$, $\eta_g = 5$. Equation 3.8 has 4 roots, but only 1 of them is physically relevant. Of the two positive roots, only one corresponds to an increase in density, temperature and entropy at the shock and thus is the physical solution. Using the values inferred from the simulations, for the case at M_A=500, I find ξ_B=0.015, that implies a solution of X=2.012, that translates into $R_{tot} = 4.05$. In the simulations with obtain a difference between the downstream and upstream density (R_{tot}) of 5, implying that the standard explanation in terms of Alfvénic fluctuations is not working, breaking then the classic MHD treatment. Another type of explanation must be found, not in term of Alfvénic fluctuations. Looking at 2(left) the magnetic field in the foot region contains many filamentary structures. These filaments are present also in the density of particle. These filaments are similar to the ones generated by the ion beam-Weibel instability, an interpretation that is worth to explore. The Weibel instability is a plasma instability present in homogeneous or nearly homogeneous electromagnetic plasmas which possess an anisotropy in momentum (velocity) space.

3.5 The dispersion equation of ion Weibel instability for magnetized plasmas with perpendicular currents

Plasma instabilities driven by currents streaming perpendicular to the ambient magnetic field play an important role in many astrophysical environments such as collisionless shocks, magnetosphere, comets, Earth's bow shock and solar wind [23]. This is exactly the configuration that I am analysing. There are many theoretical studies on this topic including also investigations of the ion Weibel instability (see [24]). The dispersion relation of plasma waves is usually calculated using a zeroth-order distribution function that satisfies the steady-state Vlasov equation, while wave-like perturbations have to satisfy the full Vlasov equation and Maxwell's equations [25]. From this system of equations it is possible to identify the growing mode of the Weibel instabilty. Authors of [26], analysing the growing mode obtained from their 2D simulations outlined that this translate into an amplification of the magnetic field in the overshock region of:

$$|B_{\rm sh}| = 2\sqrt{M_A} B_0 \tag{3.9}$$

that determines a clear dependence with M_A. I tested this prediction using the large simulations performed in the previous section. I inferred the values of the amplified magnetic field in the post shock region, computed as the average with relative standard deviation obtained at different times of the evolution of the shock, that can bring at different values of the inferred quantity due to continuous regeneration of the shock and to all the complex plasma physics occurring. The derivation of the Weibel instability described by 3.9 has to be treated as a mean behaviour of the system. Results for my setup are reported in 3.

Almost all my results are compatible within 2σ with the theoretical model inferred from the Weibel instability, pointing towards the fact that the magnetic field amplification is produced with this mechanism, that is also responible for the filamentary structure in the foot region. I find a compatibility even in the extremely high M_A regime, that was a region not yet explored previously in literature.

3.6 2D simulation: the effect of the dimensionality

Authors of [27] showed that the results obtained in 2D perpendicular shocks and the structures that are obtained can be affected by the dimensionality of the simulations in 2D; the structures when the background magnetic field lies in the simulation plane may differ from those when

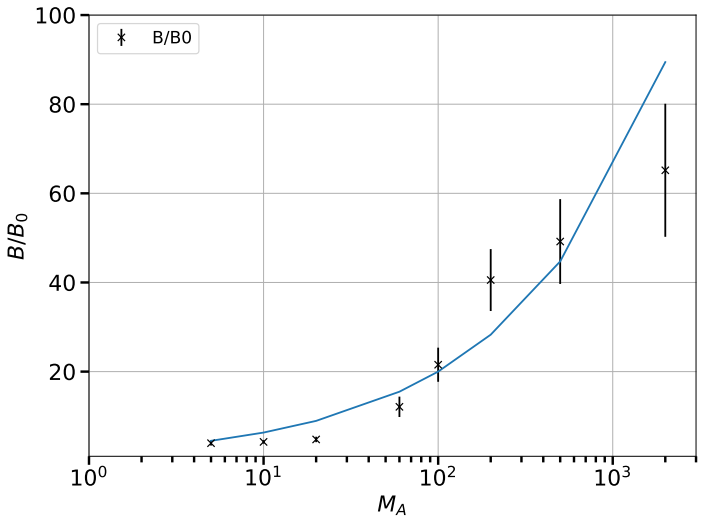

Figure 3: Ratio between downstream and upstream magnetic field magnetic field in the foot region integrated along the y direction in the whole box, computed as the average with relative standard deviation obtained at different times of the evolution of the shock for different M_A up to 2000.

it is perpendicular to the plane. Also authors of [26] outlined that electron acceleration

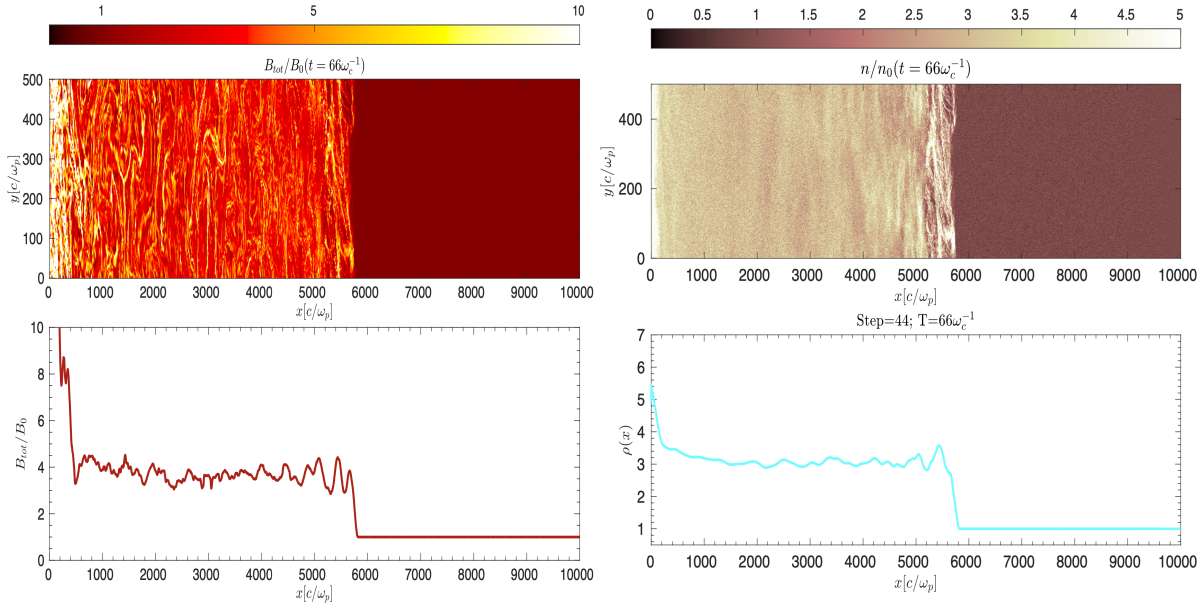

(a) (b)

Figure 4: The magnetic field amplification(left) and the particle density(right) for M_A=500. On average the magnetic field is amplified in the downstream region by a factor of ~ 4, compatible with the compression ratio obtained from right plot. The results are reported for $t = 66\omega_c^{-1}$. Evolution of she shock at later time does not change the results.

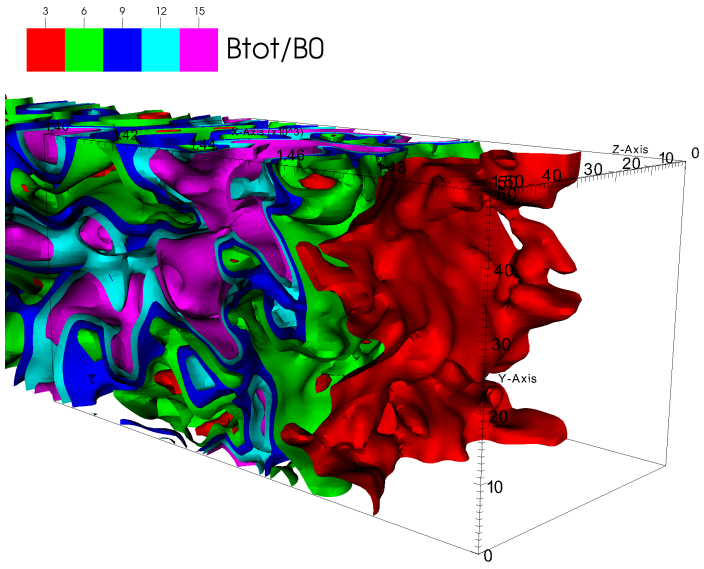

Figure 5: Ratio between downstream and upstream magnetic field for $M_A = 30$ in a 3D simulation.

is not observed in their simulations, while [20] observed a kind of electron acceleration in a perpendicular shock in their 2D PIC simulation, which used similar parameters to the one of [26]. The main reason for this is considered to be the different directions of the upstream background field: in [26] simulation it lays in the simulation plane, whereas in the simulation by [20] it is out of the plane. This again confirms the result of [27] that dimensionality can affect the results, even for 2D simulations and not only for 1D. To check what happens with hybrid simulations I also performed a test, orienting the magnetic field direction in the perpendicular plane. The results, as shown in 4 are astonishingly different. The dimensionality and the direction of the magnetic field is of fundamental importance for perpendicular shocks. Based on this I move to 3D simulations, extremely computationally expensive, but mandatory after these considerations, that can be performed only in the hybrid approach and not with PIC for reasonable timescales of evolution of the shock. I performed 3D simulations using large boxes, in order to let the shock to develop properly.

3.7 3D simulations

The problem of 3D simulations is strictly connected to the computational time, since the additional dimension increases a lot the number of processors needed for hybrid simulations. In order to obtain the maximum results in the smallest amount of time, I performed simulations in the smallest box possible and with the smallest number of particle per cell necessary. I also performed convergence tests, finding that 2.5 particle per ion skin depth is enough to not loose any type of information, with a convergence of the final results, from the value of the magnetic field amplification to the energy spectrum. In Fig. 5 I report the ratio between downstream and upstream magnetic field for $M_A = 30$ in a 3D simulation. From the color scale it is possible to find on average a magnetic field amplification downstream consistent with the Weibel predictions.

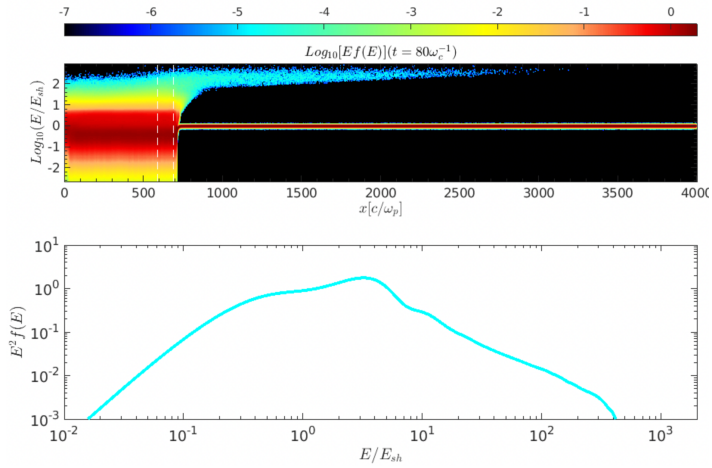

Figure 6: Energy spectrum of particles for $M_A = 30$.

3.7.1 Particle energy spectrum and acceleration mechanism

The energy spectrum is the main difference and one of the final results of this work, since for the first time in literature using self-consistent simulations of shocks I find ion acceleration in perpendicular shocks, with the presence of a non thermal tail in my results. This is a breakthrough in the field. I report in Fig. 6 for example the spectrum obtained for $M_A = 30$, where a clear non thermal tail at energies above $10 \times E_{sh}$ is present. From Fig 6 is also quite clear how the energy spectrum of particles is extremely steep, $\propto E^{-\delta}$ with values of $\delta \sim 2.7 - 3$.

The acceleration mechanism in this case deviates from the classic DSA paradigm, since particles are not able to stream freely upstream but perform giration around the magnetic field lines, that are perpendicular to the shock, so by definition, the process can't be DSA. Particles are accelerated via shock drift acceleration (SDA). The idea of SDA is that, in the reference frame of the simulation, in the upstream region particles are flowing from right to left into a magnetic field inducing a motional electric field. This electric field is able to accelerate particles that succeed in returning upstream which means that only the ions that can probe, during one gyration, the velocity jump between upstream and downstream, are accelerated via SDA, which allows some particles to gain energy quite rapidly. The energy gain per cycle is proportional to $\propto v/v_{sh}$, which means that supra-thermal particles can almost double their velocity during the first shock crossing [28]. However, in the simple SDA scenario, as also found in 2D, after a few gyrations, particles experiencing this mechanism are advected downstream, and none of them can achieve energies larger than a few times E_{sh}. However, in the simulations, since the magnetic field is enhanced downstream of the shock, particles do not penetrate far downstream, gyrating due to the direction of the magnetic field, still perpendicular to the shock direction of motion except that in a the overshoot region, where there is a partial isotropization, and some of them are actually be able to reach again the shock and jump upstream, gaining energy again via SDA. The difference between 2D and 3D can be explained by the fact that in 3D particles experience on average a positive value of the electric field in the x direction, in contrast to what I find in 2D. This quantity is able to increase the momentum of ions in the x-direction, increasing the probability of particles to reach again the shock and pass upstream. 2D simulations violate some conservation equation

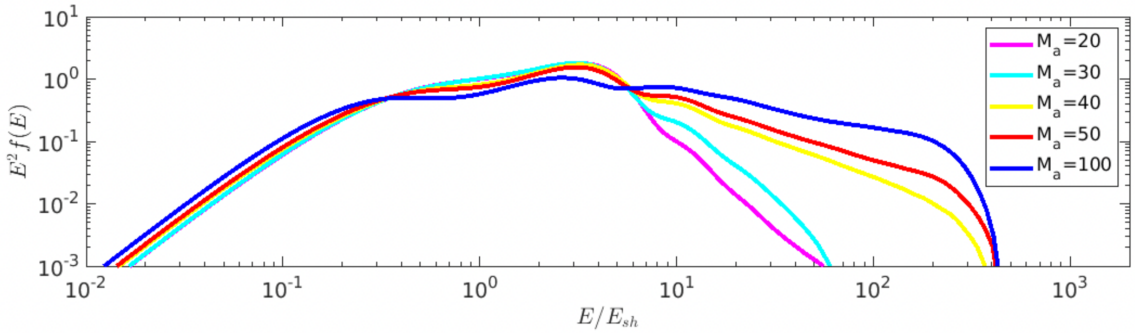

Figure 7: Energy spectrum of particles for obtained for different M_A at the same time in the simulation.

of the magnetic and electric fields, producing usually a negligible result (see for example in parallel shocks), but in this case this problem can't be ignored. In general the steepness of the spectrum with respect to the standard DSA paradigm is due to the fact that the probability of particles to satisfy the jump conditions from downstream to upstream is lower with respect to DSA, where the turbulence present after the shock isotropize particle directions of motion, sending more likely particle upstream. I also investigated the dependence of the spectrum with M_A, with the results outlined in Fig. 7. It is clear how particles with higher M_A are characterized by flatter spectra, with M_A=100 able to produce a $\delta \sim 2$. This result is obtained for two reasons: first of all, since the electric field present upstream is motional, it is proportional to $v_{sh} \times B$, so the larger is M_A the higher is the energy gain per cycle; secondly, the higher the M_A is, the larger is the magnetic field amplification downstream, factor that increases the probability to satisfy the jump conditions from downstream to upstream. Since the final spectrum is a combination between the probability of crossing the shock and the energy gain per cycle, the results found are extremely coherent.

In Fig. 8 is reported the trajectory of an accelerated particle in the x-p_x plane, performed through the tracking of ions in the simulation, where x is the x coordinate of the particle at a certain cyclotron time and p_x is its momentum in the x direction. The color scale is connected to the time of the simulation. This specific particle is gyrating upstream and downstream, gaining energy several times, until is actually able to leak out and escape upstream. The discontinuity of the trajectory point out the position of the shock at a certain time. Vertical lines also outline the position of the shock at different times. The development of a complete SDA theory for hybryd simulations will be the focus of one of the two upcoming publications. The results are consistent with some previous ones that claimed ion acceleration to be efficient at perpendicular shocks. These results have been obtained either with Monte Carlo simulations [29], or by tracking test-particles on top of the output of hybrid simulations seeded —by hand— with large-scale magnetic waves [30]. In these cases the ion scattering is prescribed (through the specification of a mean-free-path, in Monte Carlo simulations) or artificially enhanced, because of the presence of some pre-existing turbulence. My simulations, instead, allow for a self-consistent description of both the shock structure and the ion kinematics, and are long/large enough to potentially observe ions undergoing an acceleration process, for the first time in literature. This acceleration mechanism would apply also to electrons.

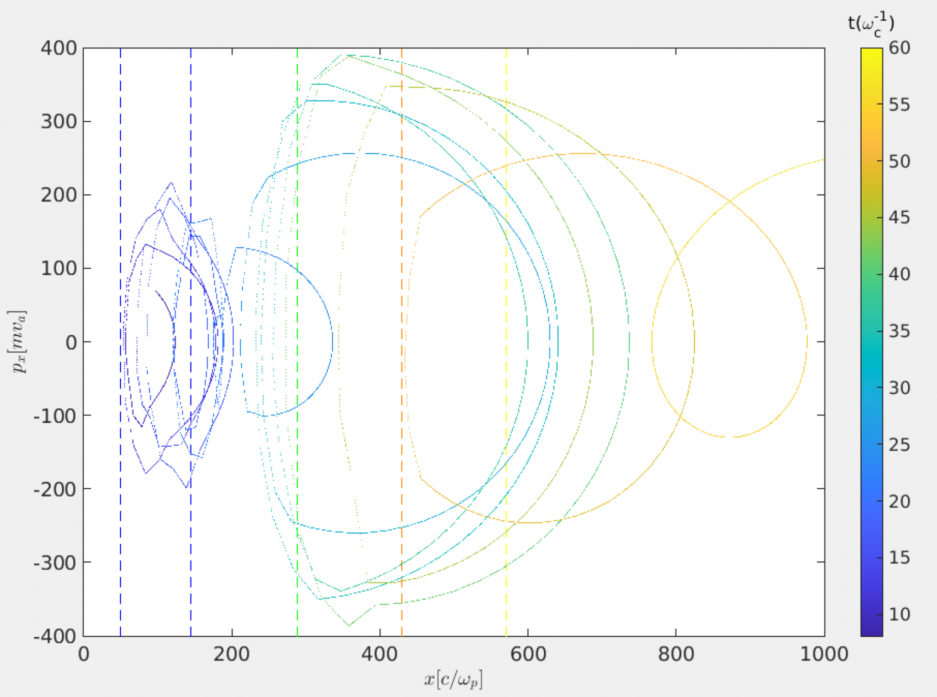

Figure 8: Trajectory of an accelerated ion in $M_A = 30$.

3.8 Remaining steps

The work performed in this two months is already a breakthrough in the field of particle acceleration in astrophysical shocks. During the first two months of my period in Chicago I explored the 2D setup, the magnetic field amplification and discovered the particle acceleration in 3D simulations. During the last months my work was affected by a slowdown due to problems of the University of Chicago cluster, that lasted for 2 weeks. In the meanwhile I started the development of the SDA theory for hybryd simulations. The remaining work planned for this part of the project is the estimation of the maximum energy of particles achieved at perpendicular shocks with different M_A, in order to study the dependence of the system from this crucial parameters. For this type of studies it is necessary for the system to develop properly in time, and so large boxes of the simulations are needed, increasing the computational demand required.

References

[1] L. Gargaté, R. Bingham, R. Fonseca and L. Silva, *dHybrid: A massively parallel code for hybrid simulations of space plasmas*, *Computer Physics Communications* **176** (2007) 419.

[2] C.C. Haggerty and D. Caprioli, *Kinetic simulations of cosmic-ray-modified shocks. i. hydrodynamics*, *The Astrophysical Journal* **905** (2020) 1.

[3] W. Baade and F. Zwicky, *On super-novae*, *Proceedings of the National Academy of Sciences* **20** (1934) 254 [https://www.pnas.org/doi/pdf/10.1073/pnas.20.5.254].

[4] E. Fermi, *On the origin of the cosmic radiation*, *Phys. Rev.* **75** (1949) 1169.

[5] W.I. Axford, E. Leer and G. Skadron, *The Acceleration of Cosmic Rays by Shock Waves*, in *International Cosmic Ray Conference*, vol. 11 of *International Cosmic Ray Conference*, p. 132, Jan., 1977.

[6] A.R. Bell, *The acceleration of cosmic rays in shock fronts – I*, *Monthly Notices of the Royal Astronomical Society* **182** (1978) 147.

[7] R.D. Blandford and J.P. Ostriker, *Particle acceleration by astrophysical shocks.*, *ApJL* **221** (1978) L29.

[8] H.J. Völk, E.G. Berezhko and L.T. Ksenofontov, *Erratum: Magnetic field amplification in Tycho and other shell-type supernova remnants*, *A&A* **444** (2005) 893.

[9] E. Parizot, A. Marcowith, J. Ballet and Y.A. Gallant, *Observational constraints on energetic particle diffusion in young supernovae remnants: amplified magnetic field and maximum energy*, *A&A* **453** (2006) 387 [astro-ph/0603723].

[10] A.M. Bykov, A. Brandenburg, M.A. Malkov and S.M. Osipov, *Microphysics of cosmic ray driven plasma instabilities*, *Space Science Reviews* **178** (2013) 201.

[11] L.O. Drury, *REVIEW ARTICLE: An introduction to the theory of diffusive shock acceleration of energetic particles in tenuous plasmas*, *Reports on Progress in Physics* **46** (1983) 973.

[12] F.C. Jones and D.C. Ellison, *The plasma physics of shock acceleration*, *SSRv* **58** (1991) 259.

[13] J. Niemiec, M. Ostrowski and M. Pohl, *Cosmic-ray acceleration at ultrarelativistic shock waves: Effects of downstream short-wave turbulence*, *The Astrophysical Journal* **650** (2006) 1020.

[14] A. Vladimirov, D.C. Ellison and A. Bykov, *Nonlinear diffusive shock acceleration with magnetic field amplification*, *The Astrophysical Journal* **652** (2006) 1246.

[15] V.N. Zirakashvili and F.A. Aharonian, *Nonthermal Radiation of Young Supernova Remnants: The Case of RX J1713.7-3946*, *ApJ* **708** (2010) 965 [0909.2285].

[16] M.A. Malkov, *Analytic solution for nonlinear shock acceleration in the bohm limit*, *The Astrophysical Journal* **485** (1997) 638.

[17] M.A. Riquelme and A. Spitkovsky, *Electron injection by whistler waves in non-relativistic shocks*, *The Astrophysical Journal* **733** (2011) 63.

[18] L. Gargaté and A. Spitkovsky, *Ion acceleration in non-relativistic shocks*, *The Astrophysical Journal* **744** (2011) 67.

[19] N. Shimada and M. Hoshino, *Strong Electron Acceleration at High Mach Number Shock Waves: Simulation Study of Electron Dynamics*, *ApJL* **543** (2000) L67.

[20] T. Amano and M. Hoshino, *Electron Shock Surfing Acceleration in Multidimensions: Two-Dimensional Particle-in-Cell Simulation of Collisionless Perpendicular Shock*, *ApJ* **690** (2009) 244 [0805.1098].

[21] L.O. Drury, *An introduction to the theory of diffusive shock acceleration of energetic particles in tenuous plasmas*, *Reports on Progress in Physics* **46** (1983) 973.

[22] D. Caprioli, E. Amato and P. Blasi, *Non-linear diffusive shock acceleration with free-escape boundary*, *Astroparticle Physics* **33** (2010) 307.

[23] T.N. Kato and H. Takabe, *Nonrelativistic Collisionless Shocks in Weakly Magnetized Electron-Ion Plasmas: Two-dimensional Particle-in-cell Simulation of Perpendicular Shock*, *ApJ* **721** (2010) 828 [1008.0265].

[24] A.L. Brinca, F.J. Romeiras and L. Gomberoff, *On the stability of perpendicular particle drifts in cold magnetoplasmas*, *Journal of Geophysical Research (Space Physics)* **107** (2002) 1090.

[25] U. Motschmann and K.-H. Glassmeier, *Dispersion and wave excitation in nongyrotropic plasmas*, *Journal of Plasma Physics* **60** (1998) 111.

[26] A. Bohdan, M. Pohl, J. Niemiec, P.J. Morris, Y. Matsumoto, T. Amano et al., *Magnetic field amplification by the weibel instability at planetary and astrophysical shocks with high mach number*, *Physical Review Letters* **126** (2021) .

[27] B. Lembège, P. Savoini, P. Hellinger and P.M. Trávnícek, *Nonstationarity of a two-dimensional perpendicular shock: Competing mechanisms*, *Journal of Geophysical Research Space Physics* **114** (2009) A03217.

[28] D.C. Ellison, M.G. Baring and F.C. Jones, *Acceleration Rates and Injection Efficiencies in Oblique Shocks*, *ApJ* **453** (1995) 873 [astro-ph/9506076].

[29] M. Baring, D. Ellison and F. Jones, *Monte carlo simulations of particle acceleration at oblique shocks: Including cross-field diffusion*, *Advances in Space Research* **15** (1995) 397.

[30] J. Giacalone and D.C. Ellison, *Three-dimensional numerical simulations of particle injection and acceleration at quasi-perpendicular shocks*, *Journal of Geophysical Research: Space Physics* **105** 12541 [https://agupubs.onlinelibrary.wiley.com/doi/pdf/10.1029/1999JA000018].